Observational studies of the meteorological characteristics associated with poor air quality over the Pearl River Delta in China

M. Wu[1], D. Wu[1,2], Q. Fan[1], B. M. Wang[1], H. W. Li[1], and S. J. Fan[1]

[1]School of Environmental Science and Engineering, Sun Yat-sen University, Guangzhou, 510275, China
[2]Institute of Tropical and Marine Meteorology, China Meteorological Administration, Guangzhou, 510080, China

Correspondence to: S. J. Fan (eesfsj@mail.sysu.edu.cn)

Abstract. The structure of the atmospheric boundary layer (ABL) and its influence on regional air quality over the Pearl River Delta (PRD) were examined through two intensive observations in October 2004 and July 2006. Analytical results show the presence of two types of typical weather conditions associated with poor air quality over the PRD. The first is the warm period before a cold front (WPBCF) and the second is the subsidence period controlled by a tropical cyclone (SPCTC). Two typical low air quality situations, which are affected by WPBCF and SPCTC, and one high air quality situation were analysed in detail. Results showed that continuously low or calm ground winds resulted in the accumulation of pollutants, and sea-land breezes had an important role during low air quality conditions. Data on recirculation factors showed that recirculation was significant during low air quality conditions, and steady transportation occurred during high air quality conditions. The ventilation index and the 24 h average ventilation index during high air quality conditions were significantly higher than those during low air quality conditions. Deep and stable inversion layers inside the ABL remarkably affected low air quality. Surface and low-altitude inversions were usually observed during WPBCF, contrary to during SPCTC, during which only the low-altitude inversion appeared frequently.

1 Introduction

The effects of the atmospheric boundary layer (ABL), an important impact factor on air quality, have been extensively investigated. Results show that meteorological processes could significantly affect air quality by controlling the time and spatial scales of pollutant dispersion (Carreras and Pignata, 2001; Cogliani, 2001; Khedairia and Khadir, 2012; Tan et al., 2009; Menut et al., 2005; Grinn-Gofron et al., 2011). Previous studies have shown that wind speed and boundary layer height are key variables in analysing the effect of ABL in the transport of pollutants (Krautstrunk et al., 2000; Davies et al., 2007). Transport of pollutants from surrounding regions also has a significant impact on city air quality (Lin et al., 2011; Wang et al., 2010). Regional emission control has become more important than local emission control in several cities (Gao et al., 2011; Schleicher et al., 2012; Zhang et al., 2012).

In addition to modern detection methods, such as sodar and radar acoustic sounding systems, tethered balloon observations are still being conducted in some areas to determine ABL structures (Neff et al., 2008; Hanna et al., 2006; Emeis et al., 2004; Alappattu and Kunhikrishnan, 2010). Data from tethered balloon observations show that light wind and lower inversion at nighttime in urban areas are important factors that contribute to poor air quality (Kolev et al., 2000; Sang et al., 2000). Weak and intermittent turbulence in nocturnal ABL and the temporary turbulent coupling of the residual layer to the surface layer facilitate the transport of pollutants, which are stored aloft over the surface (Pournazeri et al., 2012; Salmond and McKendry, 2002, Day et al., 2010).

Air pollution in urban areas has become a major issue at the Pearl River Delta (PRD) (Chan et al., 2006; Wu et al., 2007). The air pollution meteorological conditions over the PRD are different from other areas in China because the PRD faces the South China Sea to the south and is surrounded by mountains in the other directions (Fig. 1a). Tropical cyclone is a typical weather condition responsible for poor air quality over the PRD (Chen et al., 2008). Local circulations
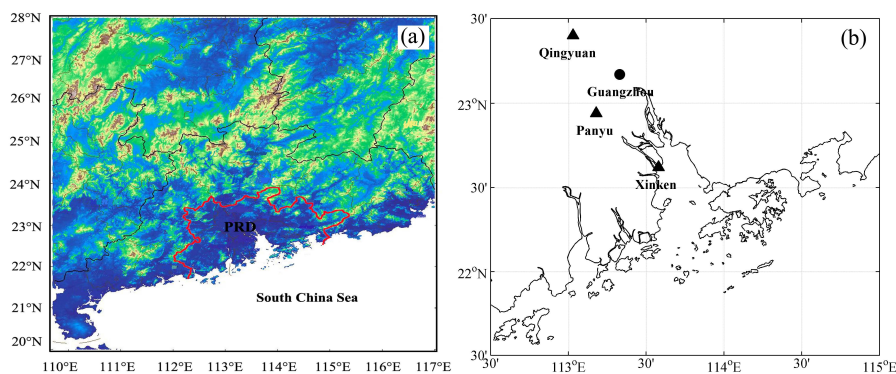
Fig. 1. Map of study area used during the PRD ABL experiment. Qingyuan, Panyu, and Xinken are the three specific sites of measurements.

such as sea-land breezes and heat-island circulation are crucial in pollution episodes (Ding et al., 2004; Fan et al., 2006). Long-range transport from regional emission sources also has an important effect on air quality over the PRD (Ding et al., 2009; Xiao et al., 2006). Tropical cyclones are important weather systems that influence the PRD during summer and autumn. Tropical cyclone subsidence reduces ABL height and produces stagnation of surface flow, thereby limiting the advection or diffusion of locally emitted pollutants (Feng et al., 2007; Wu et al., 2005). Synoptic situations and ABL structure over the PRD during summer and autumn have been discussed by Fan et al. (2008, 2011), who developed a conceptual model that shows the relationship between regional air quality and ABL meteorological conditions over the PRD (Fan et al., 2007).

The current paper focuses on meteorological characteristics associated with poor air quality over the PRD based on data from two ABL intensive observations of the Programme of Regional Integrated Experiments on Air Quality over the Pearl River Delta of China (PRIDE-PRD). We studied the weather conditions associated with the poor air quality over PRD and classified the weather conditions into different types. A comparative study was conducted on the two typical low air quality situations and one typical high air quality situation. The comparisons included differences in wind field, recirculation factor (RF), ventilation index (VI), mixing height, and sea-land breezes. An improved conceptual model of ABL associated with poor air quality over the PRD under different weather conditions was developed.

2 Experimental setup and methods

2.1 Experimental setup

PRIDE-PRD aims to characterise the pollution and improve the understanding of the chemical and radioactive processes in the atmosphere over the PRD (Zhang et al., 2008). Intensive observations were conducted in October 2004 (PRIDE-PRD 2004) and July 2006 (PRIDE-PRD 2006). In the PRD, serious pollution episodes usually occur during these seasons (Wu et al., 2007; Zhang et al., 2008).

Double-theodolite anemometry and radio soundings were used during the two intensive observations. Qingyuan, Panyu, and Xinken were selected as the observation sites (Fig. 1b). Panyu is located about 20 km south of central Guangzhou, whereas Qingyuan and Xinken are in low-urbanised environments. In addition to this intensive observation, surface measurement data, including wind speed, wind direction, temperature, and relative humidity, were collected from 27 automatic weather stations.

The Qingyuan observation station is located at the Qingyuan Meteorological Bureau. Vertical measurements were performed using meteorological radar. Mean wind speed and direction, temperature, and relative humidity were automatically derived from the radio sounding data. These parameters were obtained at 08:00, 14:00, and 20:00 LST between 0 m and 2000 m with a 100 m vertical resolution. The Panyu observation station is located at the Panyu Meteorological Bureau. Radio soundings were performed to obtain the mean wind speed, wind direction, and temperature. The position finding system of two optical theodolites was used. Radiosondes were launched seven times (06:00, 08:00, 10:00, 14:00, 18:00, 20:00, and 23:00 LST) or eleven times (intensive observation, 02:00, 06:00, *07:00*, 08:00, 10:00, 14:00, *17:00*, 18:00, *19:00*, 20:00, and 23:00 LST) per day. Mean wind speed and direction were determined between 0 m and 2000 m with a 100 m vertical resolution, whereas mean temperature was determined at a 10 m vertical resolution. The Xinken observation station is located at the 14th Bridge in Xinken. Observational methods were similar to those at Panyu.

2.2 Data and methods

We used the ventilation index (VI) and the recirculation factor (RF) to describe ventilation and recirculation.

As a useful tool for air pollution management, VI is the product of wind speed and ABL height (Pasch et al., 2011):

$$\mathrm{VI} = \sum_{i=10}^{i=\mathrm{MH}} (h_i - h_{i-1}) \cdot v_i \qquad (1)$$

where i = the level at which wind speed values were recorded, h_i = the height of level i, and v_i = the wind speed at level i.

In this study, VI was computed for each type of situation using wind data at multiple levels within the mixing layer, along with ABL height at every observation time. ABL height was estimated using the temperature profile obtained from the Xinken radio sounding measurements. Convective ABL height was considered to be the bottom of the potential temperature increase, and stable ABL height was considered to be the height of the first important variation in the vertical gradient of potential temperature (Dupont et al., 1999).

RF is the ratio of resultant transport distance to scalar transport distance (wind run). RF can be used to infer air parcel movement and the dispersive characteristics of a given air flow, such as the ventilation, stagnation, or potential recirculation of air (Allwine and Whiteman, 1994). Recirculation is an event in which polluted air is initially carried away from the source region, but subsequently returns to produce a high pollution event. When RF is equal to 1, which is a straight line, steady transport occurs. However, when RF is equal to zero, no net transport occurs, as described in Eq. (2).

$$\mathrm{RF} = \frac{(\Delta T \sum_{i_s}^{i_e} u_i)^2 + (\Delta T \sum_{i_s}^{i_e} v_i)^2}{\Delta T \sum_{i_s}^{i_e} \sqrt{u_i^2 + v_i^2}} \qquad (2)$$

where i = the time of each data point, i_s = the time of the starting data point, i_e = the time of the ending data point, ΔT = the averaging time interval of the data, u_i = x-velocity component (north was defined as the positive x axis), and v_i = y-velocity component (east was defined as the positive y axis).

The observed vertical wind data at the Xinken station were interpolated into hourly data, and then RF was calculated in each situation using the interpolated vertical wind data.

Sea-land breezes are important factors in the recirculation and trapping of air pollution. The sea-land breezes at the Xinken station are characterised by low temperature and high humidity. In this study, we used radio the sounding temperature and wind profiles at Xinken to identify sea-land breezes.

3 Weather and air quality conditions

The weather conditions during these observations were represented by changes in the daily precipitation, temperature, six-hourly wind speed, and wind direction, which were obtained from the Guangzhou Meteorological Station. Air quality during the observations was evaluated using the daily air pollution index (API) from the official website of China's Ministry of Environmental Protection. In China, API is the official index to describe city air quality conditions, and larger API values indicate worse air quality.

The time series of daily API, temperature, wind vectors, and precipitation at the Guangzhou station during the October 2004 observations are shown in Fig. 2a, c, and e. During this period, two cold fronts affected the PRD on 13 October and 28 October, which caused a significant change in wind vector and a successive decrease in temperature (Fig. 2a and c). Two periods of high API (API > 100) were also observed from 1 to 17 October and from 29 to 31 October (Fig. 2a). During these high-API periods, the wind speed was slower than $1.5\,\mathrm{m\,s^{-1}}$, and the wind direction reversed frequently. During the low-API days, wind speed was generally faster than $3\,\mathrm{m\,s^{-1}}$, and the prevailing wind directions were quite steady. Only one day of precipitation was observed at the Guangzhou station during the entire month of October (Fig. 2e).

The time series of daily API, temperature, wind vectors, and precipitation at the Guangzhou station during the July 2006 observation are shown in Fig. 2b, d, and f. During this period, two tropical cyclones affected the PRD (tropical cyclone Bilis landed on Fujian province on 14 July and tropical cyclone Kaemi landed on Fujian province on 25 July). The subsidence of these tropical cyclones resulted in a dramatic increase in temperature at the PRD (Fig. 2b and d). API also increased, as two peak API areas were found from 11 to 15 July and from 21 to 27 July (Fig. 2b). Similar to the October 2004 observations, during the high-API days of the July 2006 observations, the wind speed decreased and was generally slower than $1.5\,\mathrm{m\,s^{-1}}$ with no prevailing wind direction. During the low-API days affected by tropical cyclones the wind speed increased rapidly, accompanied with heavy rainfall (Fig. 2f), thereby decreasing API dramatically. Consequently, air quality improved.

Thus, during the 2004 and 2006 observations, four pollution episodes were observed (Table 1). The two episodes in autumn corresponded to the cold fronts, and the two episodes in summer corresponded to the tropical cyclones. According to the weather analysis of the four pollution episodes, the main weather type associated with poor air quality over the PRD could be summarised into the warm period before a cold front (WPBCF) and the subsidence period controlled by a tropical cyclone (SPCTC). During the WPBCF, the cold air was very weak. The PRD was dominated by calm wind as a result of the interaction between the cold and warm air, and regional air quality deteriorated quickly (Fan et al., 2007; Xu et al., 2011). When a tropical cyclone was close to the PRD, the subsidence was very strong, which allowed the constant accumulation of pollutants (Feng et al., 2007; Wu et al., 2005). Table 1 illustrates that polluted days during WPBCF appeared frequently during autumn. By contrast, polluted days during SPCTC appeared frequently during summer.
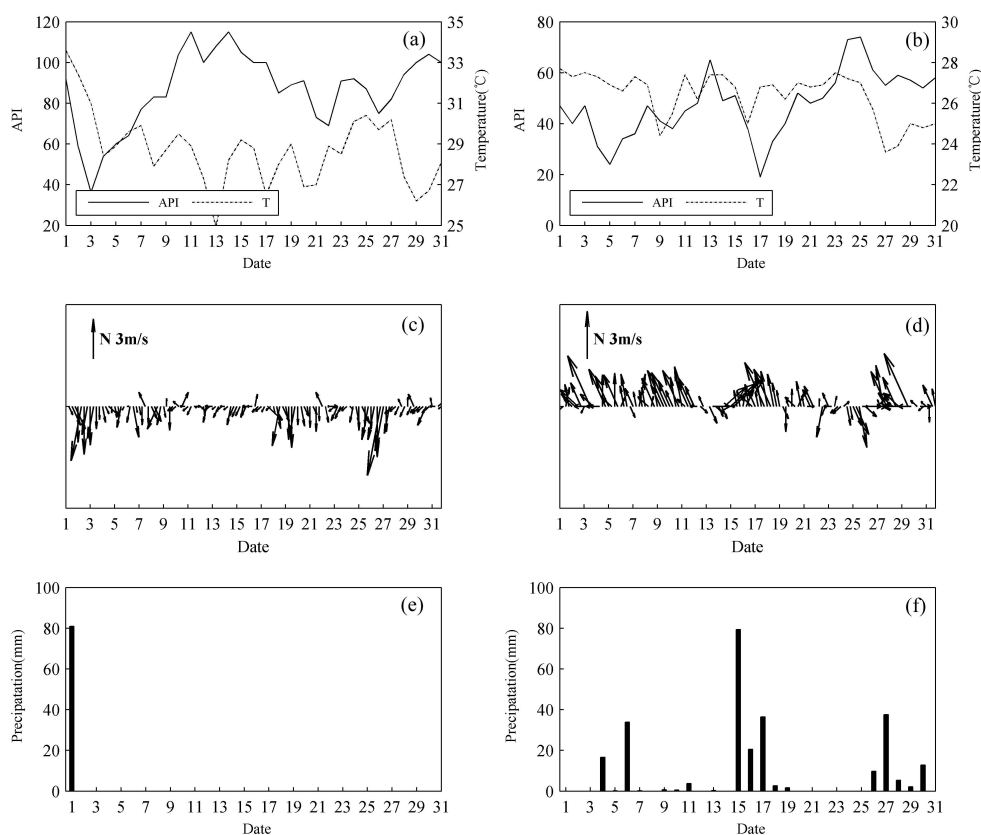
Fig. 2. Time series of **(a)** API and daily temperature from 1 to 31 October 2004 at Guangzhou station; **(b)** API and daily temperature from 1 to 31 July 2006; **(c)** six-hourly wind vectors from 1 to 31 October 2004; **(d)** six-hourly wind vectors from 1 to 31 July 2006; and daily amount of precipitation from **(e)** 1 to 31 October 2004 and **(f)** from 1 to 31 July 2006.

Table 1. Weather types of pollution episodes during the observation period.

Episode data	API feature	Weather type
10–17 Oct 2004	API > 100	In the WPBCF
29–31 Oct 2004	API > 100	In the WPBCF
13 Jul 2006	Peak API	In the SPCTC (Bilis)
23–25 Jul 2006	Peak API	In the SPCTC (Kaemi)

Based on the API and meteorological element characteristic data during the two observations, three typical situations were chosen – namely, the high-API pollution episode during WPBCF conditions from 13 to 16 October 2004, the high-API pollution episode during SPCTC conditions from 22 to 25 July 2006, and a high air quality example from 25 to 28 October 2004.

4 Results and discussion

4.1 Wind fields at the lower layers of the troposphere

The lower layer wind fields of the three typical situations were analysed using the hourly wind speed and wind direction data from 27 automatic weather stations at the PRD (Fig. 3).

During the WPBCF situation (Fig. 3a and b), the prevailing wind direction in the east PRD was opposite to that of the west PRD. The wind in the mid-area of the PRD became calm because of the convergence of the two streams. During the SPCTC situation (Fig. 3c and d), west wind dominated the north PRD and east wind dominated the south PRD, which caused the emergence of calm wind in the middle of the PRD in 23 July 2006 and in the east PRD in 25 July 2006. During the high air quality conditions (Fig. 3e and f), almost the entire PRD was dominated by a strong northeast wind on 26 October 2004. However, on 28 October 2004, the predominant wind direction of the east PRD was opposite that of the west PRD, which resulted in the occurrence of a calm wind region and increased API in Guangzhou (Fig. 2a).
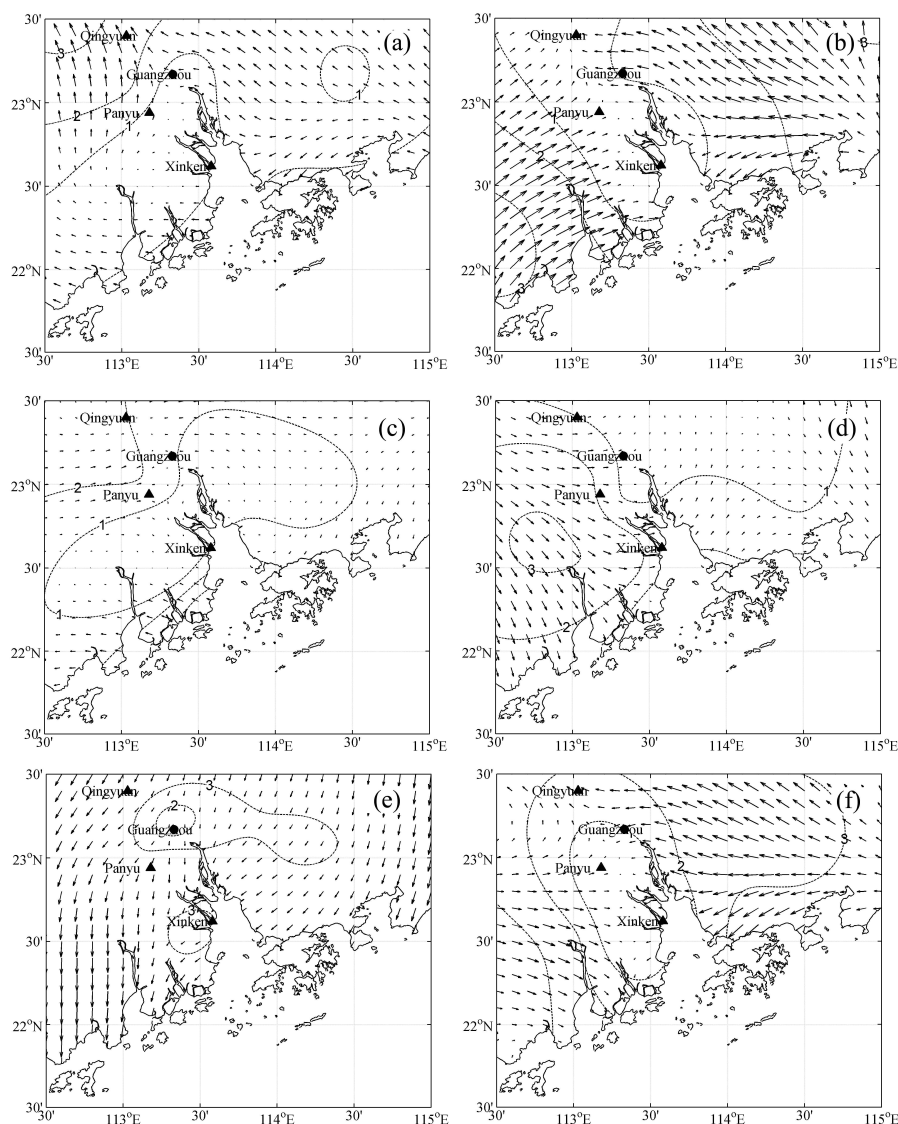
Fig. 3. Wind fields from the main meteorological stations at the PRD region. **(a, b)** 02:00 LST on 14 and 16 October 2004, **(c, d)** 02:00 LST on 23 and 25 July 2006, and **(e, f)** 02:00 LST on 26 and 28 October 2004.

During the polluted situation, the middle PRD (where Guangzhou is) was controlled by a calm wind, which resulted in poor air quality. By contrast, during high air quality conditions, the wind speed in the PRD was very strong, resulting in improved air quality.

4.2 Vertical wind

4.2.1 Vertical wind of each process

The time series of the measured vertical wind profiles of the Xinken station during the three types of weather and pollution events are shown in Fig. 4.

During the WPBCF situation (13 to 14 October 2004), the wind speed was slow with diurnal variation in wind direction below 1000 m, indicating obvious sea-land breezes (Fig. 4a). Above 1000 m, the wind profile slightly changed such that the wind direction was mostly northeastward and the wind speed was very fast, indicating that this region may be outside the ABL.

During the SPCTC situation (22 to 25 July 2006), under subsidence caused by a tropical cyclone, the lower layer wind speed was slow during the day, with diurnal variation in wind direction, indicating obvious sea-land breezes (Fig. 4b). However, the change in wind profile in the SPCTC situation was more complex than that in the WPBCF situation.

During the good air quality situation (25 to 26 October 2004), no sea-land breeze emerged under the control of fast and steady wind below 1000 m (Fig. 4c).
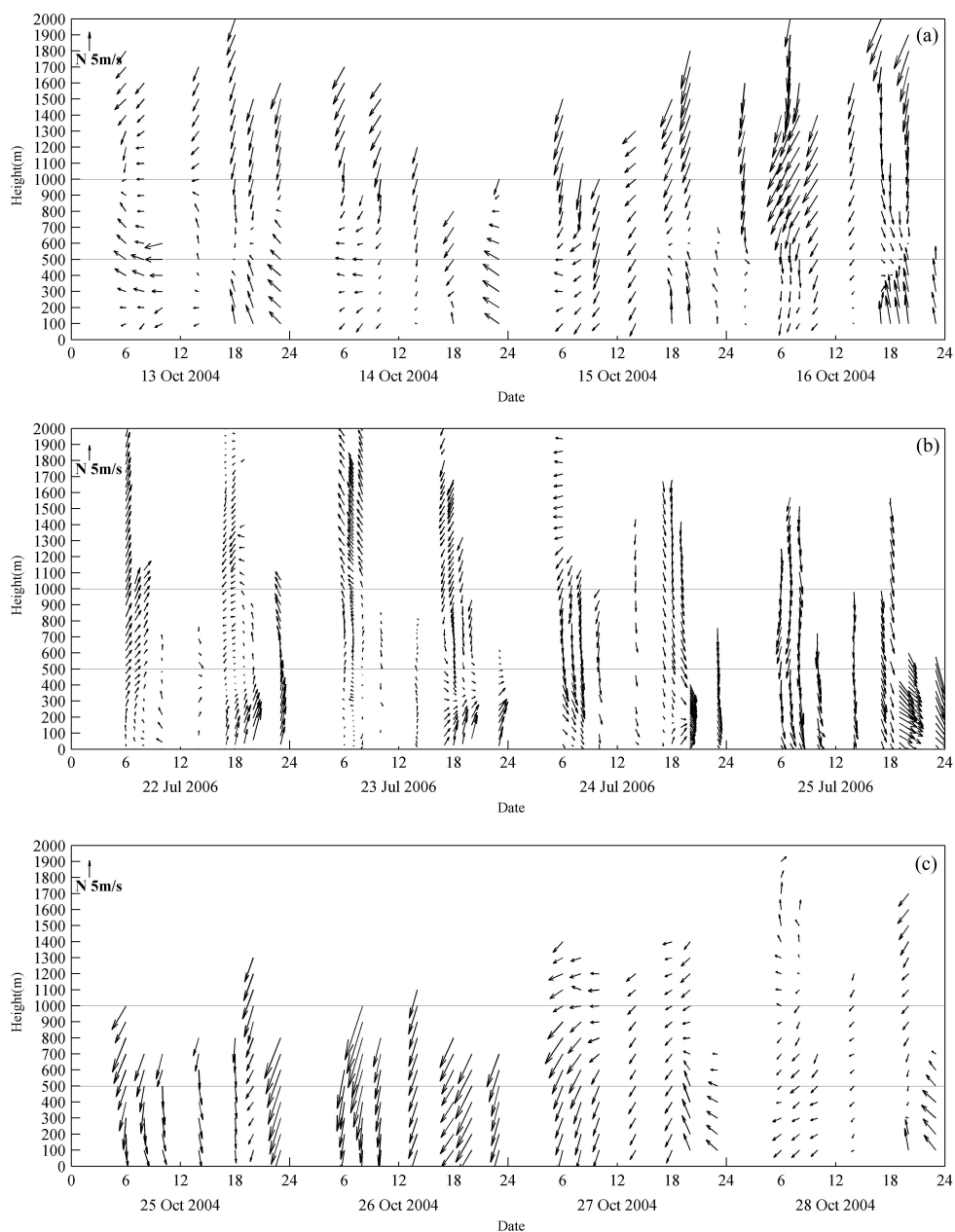
Fig. 4. Time series of vertical wind profiles at the Xinken station **(a)** from 13 to 16 October 2004, **(b)** 22 to 25 July 2006, and **(c)** 25 to 28 October 2004.

4.2.2 Diurnal variation in the vertical wind profile

Figure 5 shows the vertical wind profile and balloon trajectories obtained on 16 October 2004 while the PRD was affected by WPBCF.

The two wind shears appearing at 500 and 1000 m at the Xinken station divided the vertical wind profiles into three layers: 0 m to 500 m; 500 m to 1000 m; and > 1000 m (Fig. 5). In each layer, the vertical wind profile had remarkable differ-

ences between day and night. Especially in the low layer, the sea-land breezes were significant.

In the low layer, the land breeze emerged at 06:00 LST, with a northerly wind direction and slow wind speed. The land breeze was maintained for about 9 h. At 17:00 LST, the sea breeze emerged gradually, the wind speed increased, and the wind direction veered to the southeast. A vertical wind shear appeared and reached up to approximately 500 m at 23:00 LST due to the sea breeze.
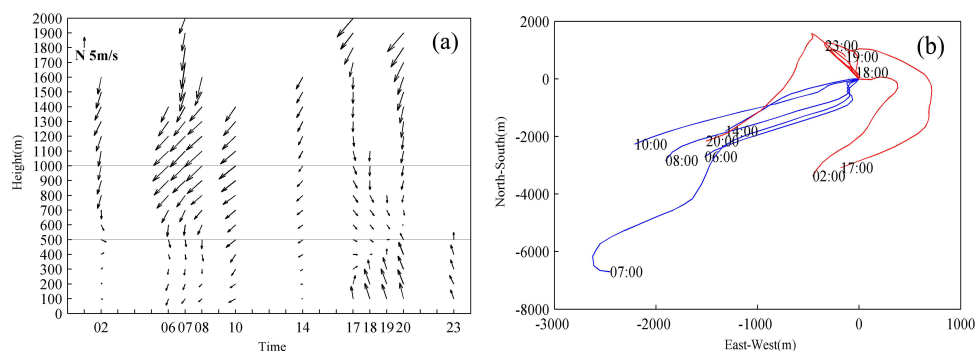
Fig. 5. Vertical wind profiles obtained by radio soundings and balloon trajectories on 16 October 2004 at the Xinken station.
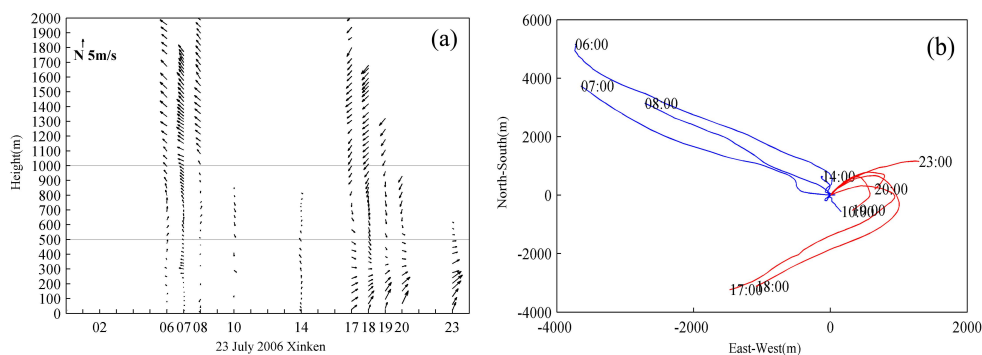
Fig. 6. Vertical wind profiles obtained using radio soundings and balloon trajectories on 23 July 2006 at the Xinken station.

In the middle layer, the diurnal variation of the wind profile was quite opposite to that of the low layer. From 06:00 LST to 14:00 LST, the wind speed increased, which corresponded to the sea breeze at high altitude, with a dominant northeasterly wind direction. After 17:00 LST, the wind speed decreased, and the wind direction veered to the northwest due to the land breeze at high altitude.

In the high layer, strong winds were observed during the entire observation period, and wind direction was northeast to north. With the influence of a sea breeze, the balloon trajectories showed remarkable reversal in direction at 17:00, 18:00, 19:00 and 20:00 LST (Fig. 5c).

The vertical wind profile and balloon trajectories obtained on 23 July 2006 while the PRD was affected by SPCTC are shown in Fig. 6.

The vertical wind profile in Fig. 6a could also be split into three distinctive layers. On 23 July 2006, given the strong influence of tropical cyclone subsidence, the wind speed was $< 3\,\mathrm{m\,s^{-1}}$ in the low layer from 06:00 LST to 14:00 LST, and the wind direction changed frequently with no prevailing wind direction (Fig. 6a). After 17:00 LST, the wind speed increased, and the wind direction veered to the west due to the sea breeze. In the middle layer, the wind speed increased along with height before 08:00 LST, while the wind direction turned from south to southeast. After 17:00 LST, the wind speed increased, and the wind direction turned to northeast.

In the high layer, a high wind speed was observed during the entire observation period. The prevailing wind direction was southeast before 10:00 LST, but it turned to the northeast after 14:00 LST.

The balloon trajectories were almost straight at 06:00, 07:00, and 08:00 LST on 23 July 2006, but, at 17:00, 18:00, 19:00, and 20:00 LST, the balloon trajectories reversed with the change in wind direction (Fig. 6b).

The vertical wind profile and balloon trajectories obtained on 26 October 2004, a day with good air quality, are shown in Fig. 7.

The wind profiles are similar most of the time (Fig. 7a), and the three-layer structure of the wind profile was not apparent (Fig. 8a). The wind speed was much faster than $5\,\mathrm{m\,s^{-1}}$ at the Xinken station, but the wind direction was very stable. The dominant wind direction was northeast. In addition, no local circulation could be distinguished.

Balloon trajectories in the high air quality conditions were completely different from those in the polluted conditions (Fig. 7b). Balloon trajectories in the high air quality situation moved southwestward and were very straight, which was consistent with the vertical wind condition.

The vertical wind characteristics of the three typical situations were compared. Results show that wind speeds in the ABL during the polluted situations were generally slower than $3\,\mathrm{m\,s^{-1}}$, and the wind direction changed frequently. At
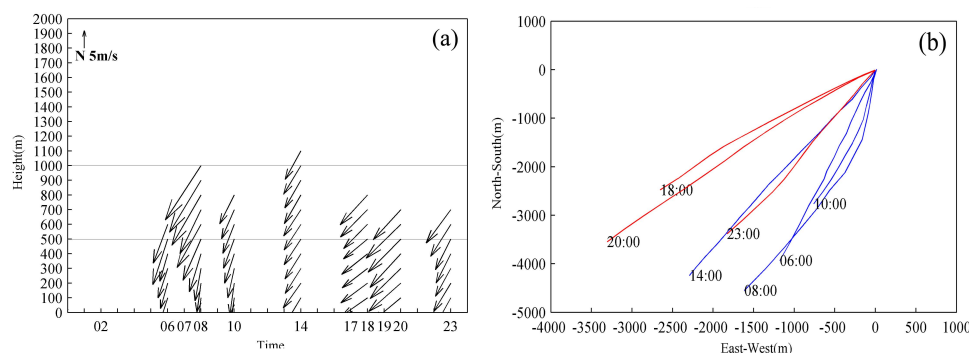
Fig. 7. Vertical wind profiles obtained using radio soundings and balloon trajectories on 26 October 2004 at the Xinken station.
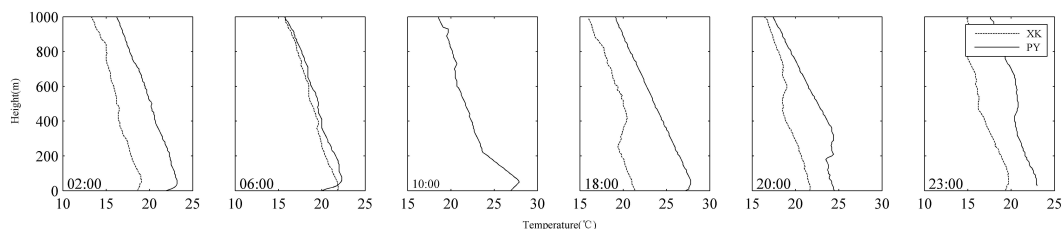
Fig. 8. Time series of vertical temperature profiles on 16 October 2004.

the Xinken station, with the influence of sea-land breezes, the pollutants were transported back to the inland areas from the coastal areas. During the good air quality situation, given the high wind speed and stable wind direction inside the ABL, the pollutants were transported and diffused effectively.

In addition, during the polluted days in which the PRD was affected by SPCTC, the subsidence flow of a tropical cyclone was important in pollutant accumulation (Chen et al., 2008; Feng et al., 2007; Wu et al., 2005).

4.2.3 Sea-land breezes

Several studies on the characteristics of sea-land breezes and their effects on pollutant transportation over the PRD have been conducted using surface measurements or model simulation (Fan et al., 2008, 2011; Zhang et al., 1999; Wang et al., 2003; Li et al., 2007; Zhuang et al., 2011). However, only a few studies on sea-land breezes of the PRD have been conducted using vertical wind data and vertical temperature data.

Sea-land breezes are mainly affected by the difference in temperature between sea and land. The variations in the vertical temperature profiles on 16 October 2004, which was a day with observed sea-land breezes, are shown in Fig. 8.

At 02:00 LST, the temperature at most of the heights measured at the Xinken station was 3 °C lower than that at the Panyu station. At 06:00 LST, the temperature at the Xinken station increased, the temperature difference between the two stations decreased, and a land breeze emerged (Fig. 5a). After 18:00 LST, the inversion layer rose to 400 m at the Xinken station because of the sea breeze, whereas the inversion layer

at the non-estuary station (Panyu) was still near the surface. At 20:00 LST, as the effect of the sea breeze reached inland, the inversion layer at the Panyu station was at 300 m and the inversion layer at the Xinken station at 600 m. At 23:00 LST, the height of the inversion layer reached its maximum at the Panyu station, but the intensity of the inversion layer weakened. At the Xinken station, the sea breeze did not further affect the inversion layer.

Table 2 shows the features of sea-land breezes at the Xinken station that were summarised from the sea-land breeze days during the observation periods. The sea breeze started at about 17:00 to 18:00 LST, with a southeast wind direction. The peak influence height was about 600 m to 800 m, which emerged at about 20:00 LST. The land breeze started at 06:00 to 07:00 LST, with a northwest wind direction. The peak influence height was 500 m to 600 m, which occurred at about 10:00 LST.

4.3 Recirculation factor and ventilation index

The vertical RFs of the three typical situations are illustrated in Fig. 9. All of the typical polluted days had a minimum value in the RF profiles. On 16 October 2004, the minimum RF was just 0.15 at about 400 m. On 23 July 2006, the minimum RF was also just 0.15 at about 700 m. The RFs during the high air quality day (26 October 2004) were larger than 0.95 at each height, which indicated that the wind direction had slight changes throughout the day. The difference in RFs indicates that recirculation was significant in the polluted situations. The pollutants were initially transported away from

Table 2. Features of the sea-land breezes at the Xinken station during the observation periods.

	Start time (LST)	Peak height (m)	Time of peak height (LST)	Wind direction
Sea breeze	17:00–18:00	600 to 800	20:00	Southeast
Land breeze	06:00–07:00	500 to 600	10:00	Northwest
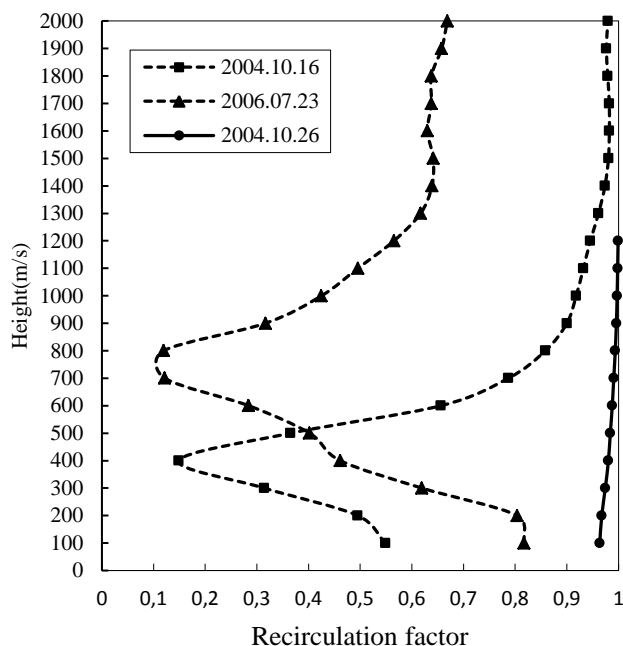
Fig. 9. RF at each height at the Xinken station on **(a)** 16 October 2004, **(b)** 23 July 2006, and **(c)** 26 October 2004.

Fig. 10. Time series for inversion layer height at the Panyu station **(a)** from 13 to 16 October 2004, **(b)** 22 to 25 July 2006, and **(c)** 25 to 28 October 2004. (Solid circles: thickness of inversion layer $\geq 100\,\text{m}$; Open circles: thickness of inversion layer $< 100\,\text{m}$)

Xinken but subsequently returned, while a steady transport occurred on the high air quality day.

Peak mixing height and VI are key ABL parameters associated with the dispersion of air pollutants. Table 3 shows the peak mixing height, peak VI, and 24 h average VI during the polluted days and the high air quality day.

The peak mixing heights were $< 700\,\text{m}$ during the WPBCF situations, whereas the peak mixing heights were $< 800\,\text{m}$ during the SPCTC situations. The peak mixing heights of the polluted days were much lower than those of the high air quality day. Lower mixing heights resulted in higher pollutant concentrations. In the WPBCF situation, the peak VI was from $184\,\text{m}^2\,\text{s}^{-1}$ to $3555\,\text{m}^2\,\text{s}^{-1}$. In the SPCTC situation, the peak VI was from $1066\,\text{m}^2\,\text{s}^{-1}$ to $4363\,\text{m}^2\,\text{s}^{-1}$. However, during the high air quality day, the peak VI was $10885\,\text{m}^2\,\text{s}^{-1}$, which was significantly larger than during the polluted days. The 24 h average VI of the polluted days was from $169\,\text{m}^2\,\text{s}^{-1}$ to $2858\,\text{m}^2\,\text{s}^{-1}$, which was also significantly lower than that during the clean day. Low VI of the polluted days was frequently associated with light winds, low mixing height, and weak transport. The poor diffusion

conditions were suitable for pollutant accumulation, which consequently caused air quality deterioration.

4.4 Inversion layer

The inversion layer is important in the pollution process. Deep and stable inversion layers inside the ABL allowed the accumulation of pollutants. The time series of inversion layer height at the Panyu station during the three typical situations are shown in Fig. 10.

Table 3. Peak mixing height, peak VI, and 24 h average VI values during the low air quality and high air quality days.

		Peak mixing height (m)	Peak VI ($m^2 s^{-1}$)	24 h average VI ($m^2 s^{-1}$)	Weather type
Low air quality days	10 Oct 2004	650	1255	930	WPBCF
	11 Oct 2004	150	184	169	WPBCF
	12 Oct 2004	650	3555	877	WPBCF
	13 Oct 2004	–	–	–	WPBCF
	14 Oct 2004	300	670	542	WPBCF
	15 Oct 2004	420	1752	1303	WPBCF
	16 Oct 2004	700	3390	1425	WPBCF
	17 Oct 2004	–	–	–	WPBCF
	29 Oct 2004	420	2014	1665	WPBCF
	23 Jul 2006	450	1066	771	SPCTC
	24 Jul 2006	700	2232	1109	SPCTC
	25 Jul 2006	800	4363	2858	SPCTC
High air quality day	26 Oct 2004	1250	10885	4084	

"–" = Invalid data in the observations.
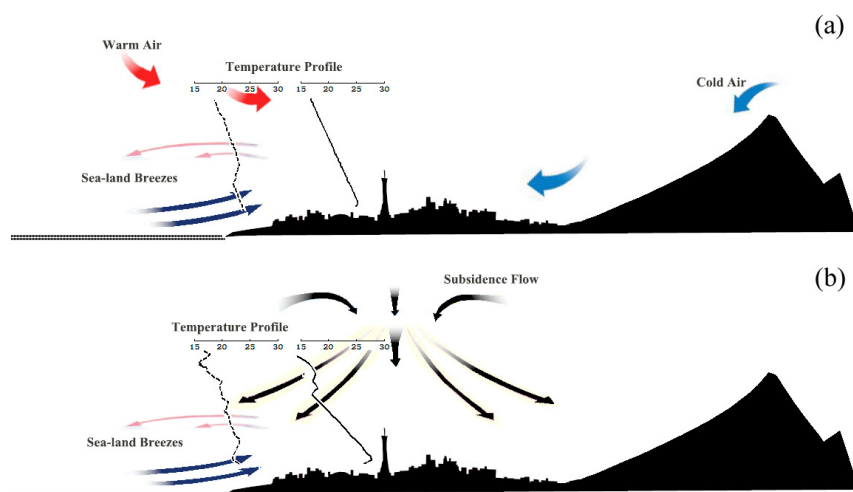
Fig. 11. Improved conceptual model of ABL influence on poor air quality over the PRD under different weather conditions.

The inversion frequency in the WPBCF situation was 76.7 %, and the surface inversion was slightly more than the low-altitude inversion (Fig. 9a). The thickness of most of the surface inversions was < 100 m, but in most of the low inversions, the thickness was > 100 m. In the SPCTC situation (Fig. 10b), the inversion frequency was 52.2 %, and most of the inversion layers occurred at low altitudes. The height of most of the low-altitude inversions were < 1000 m, and the thickness of the low-altitude inversions were high (> 100 m). In high air quality conditions (Fig. 10c), no inversion layer was observed on some days, and the inversion frequency was only 31.4 %.

5　Conclusions

Data from intensive observations showed evident differences in ABLs between low air quality and high air quality conditions.

1. The typical weather conditions associated with poor air quality over the PRD could be summarised into the warm period before a cold front (WPBCF) (Fig. 11a) and the subsidence period controlled by a tropical cyclone (SPCTC) (Fig. 11b).

2. During low air quality conditions, a calm wind region was observed over the PRD. At a near-estuary station

(Xinken), sea-land breezes were important for pollutant concentration.

3. RF is a good reference index for evaluating wind transmission capacity. A low RF was found during low air quality conditions, contrary to a high RF during high air quality conditions.

4. The peak mixing heights were < 800 m during the low air quality conditions. The peak VI of the high air quality conditions was significantly higher than those of the low air quality conditions.

5. The inversion layer inside the ABL was common during the low air quality conditions at the PRD. During the WPBCF situation, surface inversion showed a slightly higher frequency than the low-altitude inversion. However, in the SPCTC situation, low-altitude inversions had the largest proportion.

The present study provides an alternative to the conventional conceptual model, which shows the ABL characteristics associated with poor air quality over the PRD. The results are useful in developing atmospheric models and in establishing policies. The results may also serve to provide information for similar studies conducted in other places. The regional air quality over the PRD was strongly dependent on weather conditions, which are very complex and changeable. Further observational studies and numerical simulations are still necessary.

Edited by: S. C. Liu

References

Alappattu, D. P. and Kunhikrishnan, P. K.: Observations of the thermodynamic structure of marine atmospheric boundary layer over Bay of Bengal, Northern Indian Ocean and Arabian Sea during premonsoon period, J. Atmos. Sol-Terr. Phy., 72, 1318–1326, doi:10.1016/j.jastp.2010.07.011, 2010.

Allwine, K. J. and Whiteman, C. D.: Single-station integral measures of atmospheric stagnation, recirculation and ventilation, Atmos. Environ., 28, 713–721, 1994.

Carreras, H. A. and Pignata, M. L.: Comparison among air pollutants, meteorological conditions and some chemical parameters in the transplanted lichen *Usnea amblyoclada*, Environ. Pollut., 111, 45–52, 2001.

Chan, C., Tang, J., Li, Y., and Chan, L.: Mixing ratios and sources of halocarbons in urban, semiurban and rural sites of the Pearl River Delta, South China, Atmos. Environ., 40, 7331–7345, doi:10.1016/j.atmosenv.2006.06.041, 2006.

Chen, X. L., Fan, S. J., Li, J. N., Liu, J., Wang, A. Y., and Fong, S. K.: Typical weather characteristics associated with air pollution in Hong Kong area, J. Trop. Meteorol., 14, 101–104, 2008.

Cogliani, E.: Air pollution forecast in cities by an air pollution index highly correlated with meteorological variables, Atmos. Environ., 35, 2871–2877, 2001.

Davies, F., Middleton, D. R., and Bozier, K. E.: Urban air pollution modeling and measurements of boundary layer height, Atmos. Environ., 41, 4040–4049, doi:10.1016/j.atmosenv.2007.01.015, 2007.

Day, B. M., Rappenglück, B., Clements, C. B., Tucker, S. C., and Alan, B. W.: Nocturnal boundary layer characteristics and land breeze development in Houston, Texas during TexAQS II, Atmos. Environ., 44, 4014–4023, doi:10.1016/j.atmosenv.2009.01.031, 2010.

Ding, A. J., Wang, T., Zhao, M., Wang, T. J., and Li, Z. K.: Simulation of sea-land breezes and a discussion of their implications on the transport of air pollution during a multiday ozone episode in the Pearl River Delta of China, Atmos. Environ., 38, 6737–6750, doi:10.1016/j.atmosenv.2004.09.017, 2004.

Ding, A. J., Wang, T., Xue, L. K., Gao, J., Stohl, A., Lei, H., Jin, D., Ren, Y., Wang, X., Wei, X., Qi, Y., Liu, J., and Zhang, X.: Transport of north China air pollution by midlatitude cyclones: case study of aircraft measurements in summer 2007, J. Geophys. Res., 114, D08304, doi:10.1029/2008jd011023, 2009.

Dupont, E., Menut, L., Carissimo, B., Pelon, J., and Flamant, P.: Comparison between the atmospheric boundary layer in Paris and its rural suburbs during the ECLAP experiment, Atmos. Environ., 33, 979–994, 1999.

Emeis, S., Münkel, C., Vogt, S., Müller, W. J., and Schäfer, K.: Atmospheric boundary-layer structure from simultaneous SODAR, RASS, and ceilometer measurements, Atmos. Environ., 38, 273–286, doi:10.1016/j.atmosenv.2003.09.054, 2004.

Fan, S. J., Dong, J., Guo, L. L., Wang, A. Y., Somg, L. L., Liu, A. J., and Xie, J. W.: Analysis of the impact of urban growth on the tempreture field in Guangzhou, J. Trop. Meteorol., 12, 24–28, 2006.

Fan, S. J., Wang, A. Y., Fan, Q., Liu, J., Wang, B. M., and Ta, N.: Atmosphere boundray layer concept model of the Pearl River Delta and its application, J. Trop. Meteorol., 13, 8–13, 2007.

Fan, S. J., Wang, B. M., Tesche, M., Engelmann, R., Althausen, A., Liu, J., Zhu, W., Fan, Q., Li, M. H., and Ta, N.: Meteorological conditions and structures of atmospheric boundary layer in October 2004 over Pearl River Delta area, Atmos. Environ., 42, 6174–6186, doi:10.1016/j.atmosenv.2008.01.067, 2008.

Fan, S. J., Fan, Q., Yu, W., Luo, X. Y., Wang, B. M., Song, L. L., and Leong, K. L.: Atmospheric boundary layer characteristics over the Pearl River Delta, China, during the summer of 2006: measurement and model results, Atmos. Chem. Phys., 11, 6297–6310, doi:10.5194/acp-11-6297-2011, 2011.

Feng, Y., Wang, A., Wu, D., and Xu, X.: The influence of tropical cyclone Melor on PM10 concentrations during an aerosol episode over the Pearl River Delta region of China: numerical modeling versus observational analysis, Atmos. Environ., 41, 4349–4365, doi:10.1016/j.atmosenv.2007.01.055, 2007.

Gao, Y., Liu, X., Zhao, C., and Zhang, M.: Emission controls versus meteorological conditions in determining aerosol concentrations in Beijing during the 2008 Olympic Games, Atmos. Chem. Phys., 11, 12437–12451, doi:10.5194/acp-11-12437-2011, 2011.

Grinn-Gofron, A., Strzelczak, A., and Wolski, T.: The relationships between air pollutants, meteorological parameters and concentration of airborne fungal spores, Environ. Pollut., 159, 602–608, doi:10.1016/j.envpol.2010.10.002, 2011.

Hanna, S. R., MacDonald, C. P., Lilly, M., Knoderer, C., and Huang, C. H.: Analysis of three years of boundary layer observations over the Gulf of Mexico and its shores, Estuar. Coast. Shelf. S., 70, 541–550, doi:10.1016/j.ecss.2006.06.005, 2006.

Khedairia, S. and Khadir, M. T.: Impact of clustered meteorological parameters on air pollutants concentrations in the region of Annaba, Algeria, Atmos. Res., 113, 89–101, doi:10.1016/j.atmosres.2012.05.002, 2012.

Kolev, I., Savov, P., Kaprielov, B., Parvanov, O., and Simeonov, V.: Lidar observation of the nocturnal boundary layer formation over Sofia, Bulgaria, Atmos. Environ., 34, 3223–3235, 2000.

Krautstrunk, M., Neumann-Hauf, G., Schlager, H., Klemm, O., Beyrich, F., Corsmeier, U., Kaltho, N., and Kotzian, M.: An experimental study on the planetary boundary layer transport of air pollutants over East Germany, Atmos. Environ., 34, 1247–1266, 2000.

Li, M. H., Fan, S. J., Wang, B. M., Wu, D., Zhu, W., and Liu, J.: Sea-land breeze on the west coast of the Pearl River Mouth in October 2004, Acta Scientiarum Naturalium Universitatis Sunyatseni, 2, 123-125, 2007 (in Chinese).

Lin, W., Xu, X., Ge, B., and Liu, X.: Gaseous pollutants in Beijing urban area during the heating period 2007–2008: variability, sources, meteorological, and chemical impacts, Atmos. Chem. Phys., 11, 8157–8170, doi:10.5194/acp-11-8157-2011, 2011.

Menut, L., Coll, I., and Cautenet, S.: Impact of meteorological data resolution on the forecasted ozone concentrations during the ESCOMPTE IOP2a and IOP2b, Atmos. Res., 74, 139–159, doi:10.1016/j.atmosres.2004.04.008, 2005.

Neff, W., Helmig, D., Grachev, A., and Davis, D.: A study of boundary layer behavior associated with high NO concentrations at the South Pole using a minisodar, tethered balloon, and sonic anemometer, Atmos. Environ., 42, 2762–2779, doi:10.1016/j.atmosenv.2007.01.033, 2008.

Pasch, A. N., MacDonald, C. P., Gilliam, R. C., Knoderer, C. A., and Roberts, P. T.: Meteorological characteristics associated with PM2.5 air pollution in Cleveland, Ohio, during the 2009–2010 Cleveland Multiple Air Pollutants Study, Atmos. Environ., 45, 7026–7035, doi:10.1016/j.atmosenv.2011.09.065, 2011.

Pournazeri, S., Venkatram, A., Princevac, M., Tan, S., and Schulte, N.: Estimating the height of the nocturnal urban boundary layer for dispersion applications, Atmos. Environ., 54, 611–623, doi:10.1016/j.atmosenv.2012.02.024, 2012.

Salmond, J. A. and McKendry, I. G.: Secondary ozone maxima in a very stable nocturnal boundary layer – observations from the Lower Fraser Valley, BC, Atmos. Environ., 36, 5771–5782, 2002.

Sang, J. G., Liu, H. P., Liu, H. Z., and Zhang, Z. Z.: Observational and numerical studies of wintertime urban boundary layer, J. Wind. Eng. Ind. Aerod., 87, 243–258, 2000.

Schleicher, N., Norra, S., Chen, Y., Chai, F., and Wang, S.: Efficiency of mitigation measures to reduce particulate air pollution – a case study during the Olympic Summer Games 2008 in Beijing, China, China, Sci. Total. Environ., 427–428, 146–158, doi:10.1016/j.scitotenv.2012.04.004, 2012.

Tan, J. H., Duan, J. C., He, K. B., Ma, Y. L., Duan, F. K., Chen, Y., and Fu, J. M.: Chemical characteristics of PM2.5 during a typical haze episode in Guangzhou, J. Environ. Sci., 21, 774–781, doi:10.1016/s1001-0742(08)62340-2, 2009.

Wang, T., Nie, W., Gao, J., Xue, L. K., Gao, X. M., Wang, X. F., Qiu, J., Poon, C. N., Meinardi, S., Blake, D., Wang, S. L., Ding, A. J., Chai, F. H., Zhang, Q. Z., and Wang, W. X.: Air quality during the 2008 Beijing Olympics: secondary pollutants and regional impact, Atmos. Chem. Phys., 10, 7603–7615, doi:10.5194/acp-10-7603-2010, 2010.

Wu, D., Tie, X. X., Li, C. C., Ying, Z. M., Kai-Hon Lau, A., Huang, J., Deng, X. J., and Bi, X. Y.: An extremely low visibility event over the Guangzhou region: a case study, Atmos. Environ., 39, 6568–6577, doi:10.1016/j.atmosenv.2005.07.061, 2005.

Wu, D., Bi, X. Y., Deng, X. J., Li, F., Tan, H. B., Liao, G. L., and Huang, J.: Effect of atmospheric haze on the deterioration of visibility over the Pearl River Delta, Acta Meteorol. Sin., 21, 215–223, 2007.

Xiao, F., Brajer, V., and Mead, R. W.: Blowing in the wind: the impact of China's Pearl River Delta on Hong Kong's air quality, Sci. Total. Environ., 367, 96–111, doi:10.1016/j.scitotenv.2006.01.010, 2006.

Xu, W. Y., Zhao, C. S., Ran, L., Deng, Z. Z., Liu, P. F., Ma, N., Lin, W. L., Xu, X. B., Yan, P., He, X., Yu, J., Liang, W. D., and Chen, L. L.: Characteristics of pollutants and their correlation to meteorological conditions at a suburban site in the North China Plain, Atmos. Chem. Phys., 11, 4353–4369, doi:10.5194/acp-11-4353-2011, 2011.

Zhang L. F. and Zhang M.: Study of sea-land breeze system in the mouth area of the Zhujiang River, Chinese Journal of Atmospheric Sciences, 5, 581–589, 1999 (in Chinese).

Zhang, J. P., Zhu, T., Zhang, Q. H., Li, C. C., Shu, H. L., Ying, Y., Dai, Z. P., Wang, X., Liu, X. Y., Liang, A. M., Shen, H. X., and Yi, B. Q.: The impact of circulation patterns on regional transport pathways and air quality over Beijing and its surroundings, Atmos. Chem. Phys., 12, 5031–5053, doi:10.5194/acp-12-5031-2012, 2012.

Zhang, Y. H., Hu, M., Zhong, L. J., Wiedensohler, A., Liu, S. C., Andreae, M. O., Wang, W., and Fan, S. J.: Regional integrated experiments on air quality over Pearl River Delta 2004 (PRIDE-PRD2004): overview, Atmos. Environ., 42, 6157–6173, doi:10.1016/j.atmosenv.2008.03.025, 2008.

Zhuang Y. J., Wang B. G., and Liu C.: Preliminary research on the carbonyl compounds under of sea-land breeze at the west coast of the Pearl River Estuary, China Environmental Science, 4, 568–575, 2011 (in Chinese).